

Dual-arm Assembly Planning Considering Gravitational Constraints

Ryota Moriyama¹, Weiwei Wan^{12*}, and Kensuke Harada¹²

Abstract—Planning dual-arm assembly of more than three objects is a challenging Task and Motion Planning (TAMP) problem. The assembly planner shall consider not only the pose constraints of objects and robots, but also the gravitational constraints that may break the finished part. This paper proposes a planner to plan the dual-arm assembly of more than three objects. It automatically generates the grasp configurations and assembly poses, and simultaneously searches and backtracks the grasp space and assembly space to accelerate the motion planning of robot arms. Meanwhile, the proposed method considers gravitational constraints during robot motion planning to avoid breaking the finished part. In the experiments and analysis section, the time cost of each process and the influence of different parameters used in the proposed planner are compared and analyzed. The optimal values are used to perform real-world executions of various robotic assembly tasks. The planner is proved to be robust and efficient through the experiments.

Index Terms—Assembly, Dual-arm Robots, Gravitational Constraints

I. INTRODUCTION

Planning dual-arm assembly of multiple objects is a challenging problem. During the assembly, one of the robot arms holds the finished part, and the other arm assembles the next part to it. To automatically plan the assembly motion, one needs to consider the grasp configurations, the assembly positions and orientations, the constraints from the start and goal poses of the object parts, the kinematic constraints of the robots, as well as the gravitational constraints of the finished part. While these problems were previously studied independently or partially, they are not analyzed and developed as an integral planner for dual-arm multi-object assembly.

Under this background, this paper develops an integral planner to plan the dual-arm assembly of more than three objects. The planner automatically generates the grasp configurations for each object and the assembly positions and orientations in the work space. The grasp configurations and assembly positions/orientations are sampled from a grasp space and an assembly space. The proposed planner simultaneously searches and backtracks the grasp space and assembly space to accelerate the motion planning of robot arms.

Especially, the proposed planner is able to deal with the planning of more than three objects by considering gravitational constraints. Gravity may break the finished part when the holding hand changes its pose without considering the gravitational constraint. Fig.1(a) shows an example. The

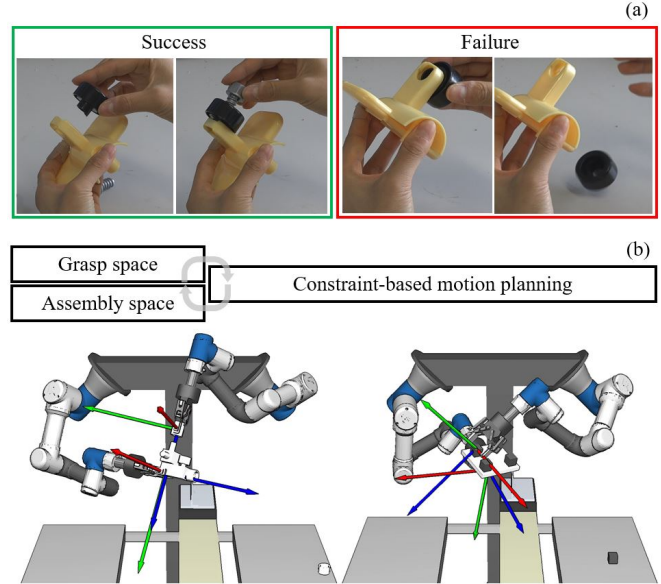


Fig. 1: (a) In the left part, the holding hand keeps the yellow object tilted to support the wheel. The bolt is thus successfully assembled. In the right part, the wheel drops down due to pose changes and gravity. (b) Upper part: The workflow of the proposed planner; Lower part: Two exemplary keyposes from the planned motion.

left part shows a successful assembly motion where the holding hand kept the yellow object tilted to support the wheel. The left hand could release and continue to assemble the bolt. In contrast, the right part shows a failure motion. In this case, the left hand moved, the wheel dropped down, and the finished part was broken. The planner proposed in this paper aims to avoid the failure happened in the second case by considering gravitational constraints.

Fig.1(b) shows an overview of the proposed planner. It loops through the grasp space and assembly space (the contents in the left two boxes in the upper part of Fig.1(b)) to search and backtrack the grasp configurations and assembly poses of dual-arm assembly. Especially during the motion planning (the right box in the upper part of Fig.1(b)), the planner considers both collision and gravitational constraints to not sample problematic nodes and ensure safe motion.

In the experiments and analysis section, the time cost of each process and the influence of different parameters used in the proposed planner are compared and analyzed. The optimal values are used to perform real-world executions of various robotic assembly tasks. The planner is proved to be robust and efficient through the experiments.

¹Graduate School of Engineering Science, Osaka University, Japan.

²National Inst. of AIST, Japan. *Correspondent author: Weiwei Wan: wan@sys.es.osaka-u.ac.jp

II. RELATED WORK

The related studies of this work include: classic assembly planning, robotic task and motion planning, and dual-arm manipulation.

A. Classic assembly planning

The seminal studies in classic assembly planning focused on the high-level geometric reasoning of CAD models [1] [2] [3]. The goal was to generate the order in which parts come together. Similar following studies include [4] [5] [6]. These early assembly planning studies used mostly geometric constraints.

More recent planners tend to use a mixed model of constraints. The seminal studies of classic assembly planning were extended by considering gravitational constraints and the mutual support between objects in the 1990s [7], and lots of studies were inspired by the extension. For example, Dobashi et al. [8] considered both geometric and grasp constraints to assemble wooden blocks. Dogar et al. [9] used both geometric and grasp constraints to assemble chairs. Suarez-Ruiz et al. [10] presented a similar chair-assembly task, where force control was further included to finish the precise insertion. MacEvoy et al. [11] considered the stability and geometric constraints to plan assembly sequences of truss structures. A survey that summarized the work that considered various constraints before 2015 is available in [12]. In our recent work [13], a mixed constraint of stability, graspability, and assemblability was used to plan the robot motion to assemble Soma cubes.

This paper assumes the order of assembly is given. It does not re-implement a classic assembly planner that uses various constraints to optimize assembly orders. Instead, the constraints are considered during the planning of grasp configurations, assembly poses, and robot motion, which is more like the task and motion planning that follows.

B. Task and motion planning

Task and motion planning (TAMP) plans the robotic motion to manipulate parts considering geometric constraints and task orders [14]. It includes but is not limited to assembly.

Modern TAMP planners use a symbolic reasoner to find task-level jobs, and iteratively runs motion planning to find the robot motion for each job. For example, Wolfe et al. [15] used HTN (Hierarchical Task Networks) to divide and conquer sub-planning problems. Srivastava et al. [16] interweaved PDDL (Planning Domain Description Language) and RRT (Rapidly-exploring Random Trees) to plan a motion to arrange a cluttered table. Zhang et al. [17] used multi-level optimization, incorporating task, action, and motion planning, to generate a combined motion plan for a mobile manipulator. Recently, Lagriffoul et al. [18] proposed a benchmark for TAMP planners. The benchmark includes not only mobile pick-and-place tasks but also assembling parts at a stationary position.

The planner developed in this paper is one kind of TAMP planner. Compared to the other TAMP planners, our main

contribution is planning the pick-and-assembly motion of multi-objects using dual-arm robots.

C. Dual-arm manipulation

Dual-arm manipulation and dual-arm manipulators are popular topics in robotics and are widely studied [19] [20]. Most of the dual-arm manipulation planning studies focus on sequential manipulation [21] [22] [23] and coordinated dual-arm motion planning [24] [25]. Dual-arm assembly is less studied. The most recent dual-arm assembly work we could find is [26], which used dual-arm robots to assemble two parts considering motion and force capabilities.

This paper develops a dual-arm assembly planner. The difference from previous dual-arm manipulation studies is the consideration of multiple parts and gravitational constraints. An integral and practical planner for dual-arm multi-object assembly is implemented.

III. OVERVIEW OF THE METHOD

This section gives a general explanation of the proposed method. The rough idea is already mentioned in the upper part of Fig.1(b), which iterates through the grasp space and assembly space to get the start and goal configurations for sampling-based motion planning. The detailed workflow is shown in Fig.2.

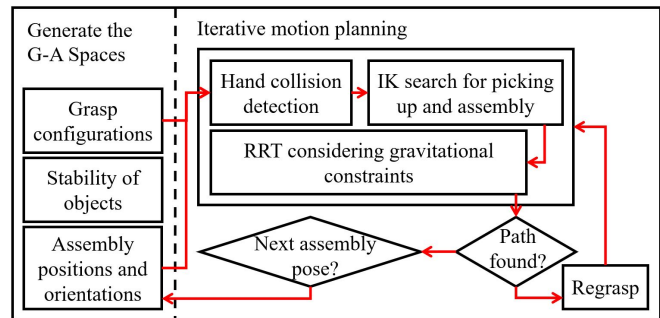


Fig. 2: Detailed workflow of the proposed method. It iterates through the grasp space and assembly spaces (G-A spaces) to get a sequence of start and goal configurations for RRT. In case no path is found, the method tries the next assembly positions and orientations, or refers to regrasp to reorient the initial poses of the parts.

First, the method generates the grasp and assembly spaces (G-A spaces) by synthesizing grasp configurations and assembly poses, as is shown in the left part of Fig.2. The details of the synthesizing will be discussed in Section IV. The stability of the parts, namely the stable placements of the parts on tables, is also computed to allow the robot to reorient them using regrasp planning [22].

The right part of Fig.2, namely the iterative planning part will search the G-A spaces to get a sequence of start and goal configurations for RRT motion planning. If the sequence of start and goal configurations could be found, the planner will call gravity-constrained RRT to plan robot motion between each adjacent start and goal in the sequence. If the sequence is not available, the planner will iterate to the next assembly

pose, and re-search. The method reports a successful plan if all robot motion between the adjacent start and goal configurations in a sequence could be found. The details of iteration and gravity-constrained RRT will be discussed in Section V. Especially, two different algorithms were proposed to select the start and goal configurations. These two algorithms are compared in detail in the experiments and analysis section.

IV. THE GRASP AND ASSEMBLY SPACES (G-A SPACES)

The grasp space is defined as a space of hand poses that can hold an object in force closure. We use a grasp synthesis method proposed in [27] to compute the grasp space of an object. The method is able to plan precise grasp poses for suction cups and parallel grippers. The basic idea is to find planar facets, sample the facets, and find the candidate samples for attaching suction cups or gripper finger pads. The method provides several tunable parameters to control the density of the synthesized grasp configurations. By using this method, we can automatically compute a lot of candidate grasps using the CAD model of an object. Fig.3 shows some grasp configurations synthesized by the method. They are discretized samples from the grasp space.

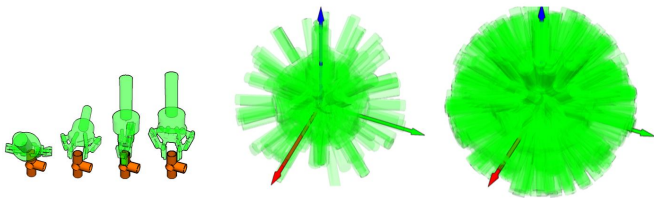


Fig. 3: Some grasp configurations sampled from the grasp space. The left figure shows several independent grasp configurations. The middle and right figures show two final results. The middle one has a smaller number of synthesized grasp configurations than the right one. The number of grasps could be controlled by tuning the parameters provided by the grasp synthesis method.

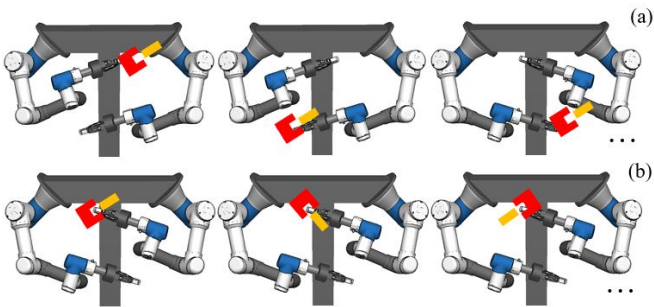


Fig. 4: Assembly positions and orientations. The robot may assemble the yellow peg and the red slot at lots of different positions shown in Fig.4(a), as well as lots of different orientations shown in Fig.4(b).

The assembly space is defined as a space of positions and orientations for the dual-arm robot to assemble two objects. Fig.4 shows an example. The dual-arm robot may

assemble a yellow peg and a red slot at lots of different positions shown in Fig.4(a), as well as lots of different orientations shown in Fig.4(b). These different positions and orientations are discretized samples from the assembly space. To plan these discrete assembly positions and orientations, random sampling together with icospheres are used. First, we discretize the candidate assembly region by defining an area in front of the dual-arm robot, and sample the assembly region to get several assembly positions. Then, at each sampled position we sample the assembly orientations by using icospheres (see the left part of Fig.5(a)). The vector pointing to each vertex of an icosphere is used as the z axis of an assembly orientation (blue vectors in the right part of Fig.5(a)). The x and y are sampled around the z axis to finalize the rotation frames (the red and green vectors in the right part of Fig.5(a)). Different levels of icospheres are used and analyzed in the experiments and analysis section to show their influence on the performance of the proposed planner. Fig.5(b) shows an example where a shaft and bearing in the left part is sampled to be assembled at the many candidate orientations shown in the right. These candidate orientations are obtained from the rotation frames shown in Fig.5(a).

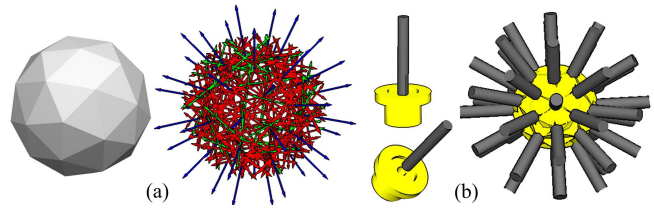


Fig. 5: (a) Left: A level-1 icosphere. Right: The assembly orientations obtained by defining rotation frames using the vectors pointing to the vertices of the icosphere. (b) An example where the shaft and bearing in the left part is sampled to be assembled at the many candidate orientations shown in the right.

V. MOTION PLANNING BY INTERACTING WITH THE G-A SPACES

A. Assembling the first two objects

After sampling the G-A spaces and obtaining the discretized grasp configurations and assembly poses, the proposed method starts iterating through them to get a sequence of key robot poses and plan the robotic assembly motion. The right part in Fig.2 roughly shows the workflow of the iteration. First, the “Hand collision detection” frame box will select some candidate grasp configurations and an assembly pose from the discretized G-A space. All the objects, the surrounding obstacles, and the kinematics of the robot are considered during the selection. The candidate collision-free grasp configurations for objects both at the initial pose and the assembly pose will be obtained after the selection. An exemplary result is shown in Fig.6. In the left part, a bearing is at its initial pose on a table. The “Hand collision detection” frame box selects the green hands as the candidates to pick up the bearing. The blue hands are the collided hands and are removed. In the right part, the “Hand collision detection”

frame box selects one assembly pose and finds the collision-free grasp configurations to assemble the parts. The red hands are the candidates grasp configurations for the right hand. The blue hands are the candidate grasp configurations for the left hand. The proposed method will solve the IK for the candidate grasp configurations and use the found robot poses as start and goals for RRT motion planning. They are carried out in the “IK search for picking up and assembly” frame box, and the “RRT considering gravitational constraints” frame box.

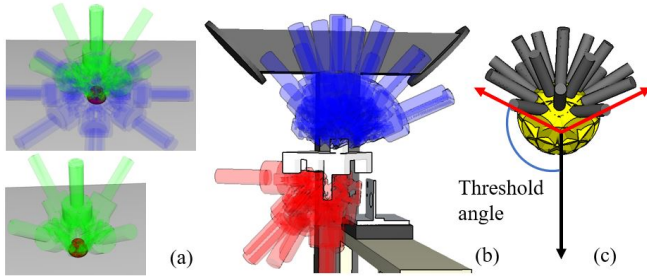


Fig. 6: (a) Selecting the grasp configurations to pick up an object from its initial pose. The green hands are the selected grasps. (b) Selecting an assembly pose and finding the collision-free grasp configurations for the two hands.

The order to perform the selection is crucial to the time cost. There are two ways to implement the order. They are shown in Fig.7 and Fig.8 respectively. The two parts in the assembly are named part 1 and part 2. In the first case, the algorithm works as follows.

- (1) The algorithm chooses a candidate assembly pose from the assembly space.
- (2) For part 1, the algorithm computes the “candidate grasps to assemble part 1” and the “candidate grasps to pick up part 1” from its initial pose.
- (3) The algorithm computes the intersection of the “candidate grasps to assemble part 1” and the “candidate grasps to pick up part 1”, and finds a set of collision-free and IK-feasible grasps from the intersection.
- (4) For each grasp in the set, the algorithm repeats (1)-(3) for part 2, avoiding not only the collision with the parts, but also the collision with the candidate grasp of part 1. The algorithm stops if a feasible grasp for part 2 is found.

The workflow of the second algorithm is as follows.

- (1-3) The same as the first algorithm.
- (4) The algorithm performs (3) and (4) for part 2.
- (5) The algorithm merges the CD-free and IK-feasible grasps of part 1 and part 2 by pairing them. The algorithm returns the first pair for future use.

The first algorithm repeatedly performs collision detection for each of the selected grasps for part 1. The advantages of the algorithm is it may quickly find a pair of candidate grasps for the two parts if a solution exists and the random search is lucky. In contrast, the second algorithm computes the collision-free and IK-feasible grasps for both part 1 and

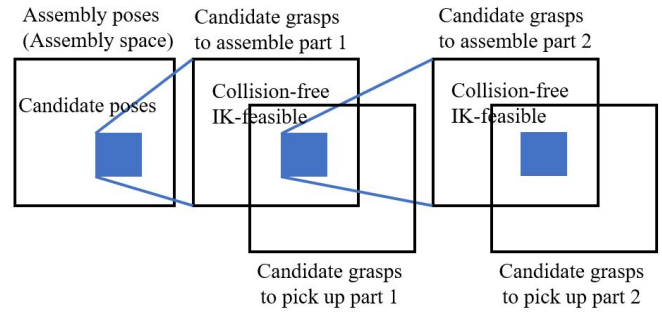


Fig. 7: The first way to select the grasps for assembly.

part 2 in the second, and uses a pairing step to merge them. It is faster to find all pairs of candidate grasps, but is slower to get a single one since all grasps for the two parts have to be examined before getting the results. Both the two algorithms are implemented in our planner. Their performance is compared in the experimental section.

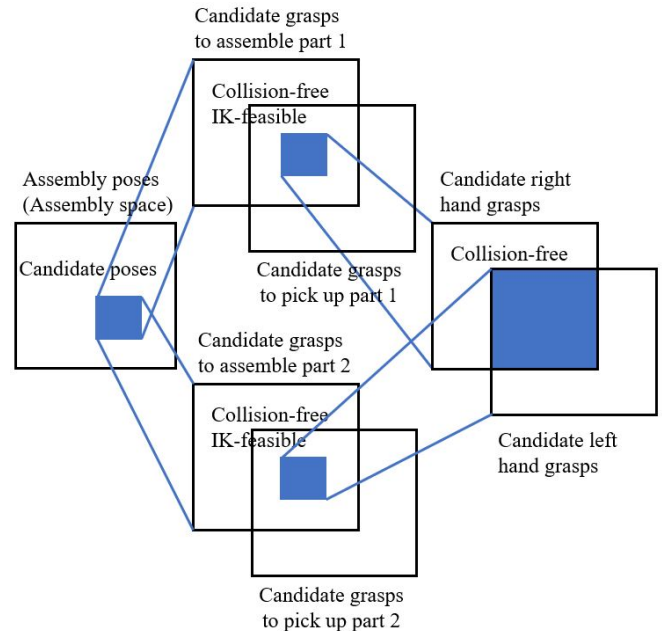


Fig. 8: The second way to select the grasps for assembly.

In the two-object assembly, we do not really need to consider gravitational constraints during motion planning since all objects are held firmly by the two hands. We only need to consider gravity when choosing the candidate assembly poses (the first step of the two algorithms) – Part 2 must be supported by part 1 to avoid dropping down. This constraint is defined as an angle between the assembly direction and gravitational direction. When the angle is smaller than a value, the assembly is considered to be unstable. The assembly poses of the peg and bearing, after considering the gravitational constraints, are shown in Fig.6(c). The peg never points downward.

B. Assembling the remaining parts

When assembling the third part, part 1 and part 2 are assembled together. They become a finished part. The goal of assembly is to assemble part 3 to the finished part (namely part 12). The selection of candidate grasps and the motion planning for the arm holding part 3 is the same as the two-object assembly. The motion planning for the arm holding part 12 needs to be carefully designed considering the gravitational constraints. Our implementation is the gravity-based motion planning illustrated in Fig.9. It is a variation of RRT motion planning. When sampling a new node, the gravity-based planner not only check the collision of the node and the edge with the configuration obstacles, but also the stability of the finished part. The gravity-based planner ensures that part 2 will be supported by part 1 to avoid falling down.

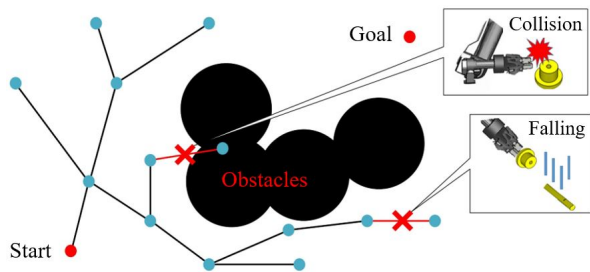


Fig. 9: Gravity-based motion planning. Both collision and the gravitational constraints are examined when a new node is sampled during the motion exploration.

The gravitational constraint is also implemented as the angles between constraint vectors. Assume the assembly direction of part 12 is denoted by v_{a12} . The gravitational constraint is to require the angle between v_{a12} and gravitational direction to be larger than a threshold. If the angle is too small, the assembly is considered to be unstable. For the 4th, 5th, etc., objects, the gravitational constraint is met when all angles between the assembly directions and gravitational direction are larger than the given threshold.

VI. EXPERIMENTS AND ANALYSIS

We developed both simulation and real-world experiments to examine the proposed planner. Two sets of assembly tasks, shown in Fig.10 were used for analysis. The first set was to put two rings on a branched base. The rings were quite loose. A robot must not let any branch face downward during assembly. The second set was to place four blocks onto a plate. A robot had to keep the plate facing upward to avoid losing finished blocks. The computational platform used in the experiments was a PC with Intel Core it-6500 CPU and 8.00GB memory. The programming language was Python 2.7. The software platform was Pyhiro¹.

The results of simulation and real-world execution are shown in Fig.11. For the first assembly set, the robot chose to assemble the first ring from an upward direction, as is shown

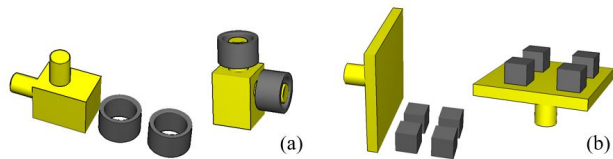


Fig. 10: Two sets of assembly tasks used in the experiments. The first task is to assemble one base and two rings shown in the left part of (a) to the right state. The second task is to place four blocks onto a plate.

in Fig.11(a-3,4). Before assembling the third ring, the robot rotated the finished part in Fig.11(a-5) while successfully avoided losing the first ring. The gravity-constrained planner was acting an important role in producing the motion. For the second assembly set, The robot was maintaining the upward pose of the plate in Fig.11(b-3,4,5,6). At the same time, it was also computing the optimal pose for assembly motion. In Fig.11(b-3,4,6), robot was holding the plate horizontally. In Fig.11(b-5), the robot tilted the plate a bit to let its left arm easily access the goal dropping position. The gravity-constrained planner optimized the assembly poses automatically.

The parameters used in the experiments are shown in Table I. The number of sampled grasp configurations for the right and left arms was 200 and 234 respectively. The number of sampled assembly positions was 4. The number of sampled assembly orientations was 252 (icosphere level 2). The angle threshold for the first assembly set was 90° . It required the angle between a branch and the gravitational direction to be larger than 90° . The angle threshold for the second assembly set was 175° . It required the angle between the upward direction of the plate and the gravitational direction to be larger than 175° . The second selection algorithm mentioned in Section V-A was used.

TABLE I: The parameters used in the experiments

G space	# of sampled grasps (right-left)	200 · 234
A space	# of sampled assembly positions	5
	# of sampled assembly orientations	14913
Grav. cstr.	Set 1: 90°	Set 2: 175°
Sel. ord.	Order 2	

of sampled grasps (right-left): # of right hand · # of left hand; Grav. cstr. - Gravity constraint; Sel. ord. - Selection order.

The computational costs to plan the assembly motion for the two sets are shown in Table II. The time is the mean of ten times of simulation. The problems could be solved safely with less than 1 minute, using pure Python.

Besides the chosen parameters shown in Table I, various other candidates were tested. The computational costs under the other settings and the detailed costs of each process in the planner are shown as follows. First, for the two selection orders mentioned in Section V-A. The costs are shown in Table III. The second order was more stable when the random search was not lucky. Also, the second order produced more

¹<https://github.com/wanweiwei07/pyhiro>

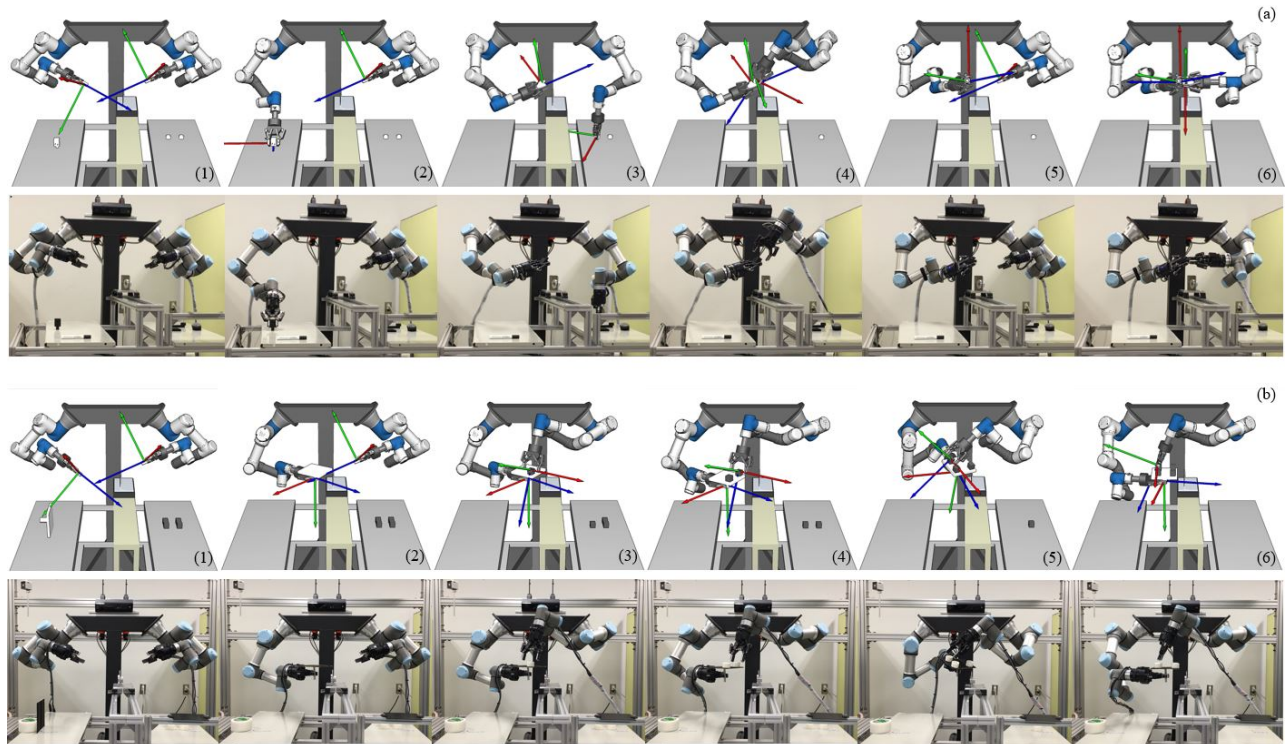


Fig. 11: Two sets of assembly tasks used in the experiments. The first task is to assemble one base and two rings shown in the left part of (a) to the right state. The second task is to place four blocks onto a plate.

TABLE II: Time costs of the two assembly sets

	Set 1	Set 2
First assembly pose and IK	34.95 <i>s</i>	12.34 <i>s</i>
The remaining assembly poses and IK	18.23 <i>s</i>	7.84 <i>s</i>
First gravity-constrained RRT	42.74 <i>s</i>	21.73 <i>s</i>
The remaining gravity-constrained RRT	26.58 <i>s</i>	17.69 <i>s</i>

The time costs in the table are the mean of ten simulation.

flexible right-left combinations than the first order. Multiple right grasps were paired with multiple left grasps. In contrast, one right grasp was paired with multiple left grasps in the first order. Thus, the second selection algorithm was used.

TABLE III: Comparison of the two selection orders

	Set 1	Set 2
With IK-feasible grasps	1.14 <i>s</i>	6.31 <i>s</i>
IK-feasible at the 10th trial	150.17 <i>s</i>	88.96 <i>s</i>
Candidate pairs (right-left)	1-n	m-n

The time costs in the table are the mean of ten simulation.

The time costs with respect to different G-A space samples are shown in Table IV. The left column is the number of sampled assembly positions. The upper row is the number of sampled grasps. As the number of grasps increased, the time costs got much larger. On the other hand, the number of assembly positions did not significantly increase

the computational load. For this reason, we used 4 in the experiments.

TABLE IV: Comparison of the two selection orders

# posn.	# of sampled grasps (right · left)				
	200 · 234	256 · 348	320 · 456	420 · 614	596 · 772
3	NA	91 <i>s</i>	124 <i>s</i>	144 <i>s</i>	212 <i>s</i>
4	90 <i>s</i>	94 <i>s</i>	130 <i>s</i>	149 <i>s</i>	227 <i>s</i>
5	92 <i>s</i>	101 <i>s</i>	133 <i>s</i>	152 <i>s</i>	249 <i>s</i>

The time costs in the table are the mean of ten simulation.

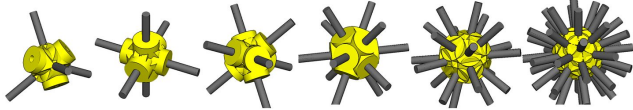
The detailed costs and discovery rates for different numbers of assembly orientation are shown in Table V. Here, different levels of icospheres are used to generate the assembly poses. The correspondent illustrations of the different levels are under the table. The results showed that the success rate increased as the number of orientation increased. Meanwhile, there was no significant change in the time cost before finding feasible assembly motion by random search. Thus, we used the highest number of orientation, 252, in the results shown in Fig.11.

Finally, the detailed costs of each process in the planner with respect to different numbers of sampled grasps are shown in Table VI. Here, the number of assembly positions was 4. The number of assembly orientations was 252. Of all the process, the CD (collision detection) costed the most computational resources. The IK costs increased significantly as the number of grasps increased. The RRT did not change much with more grasps. Besides the presented results, read-

TABLE V: Comparison of different # of assembly orientation

Icosphere level	# orien.	t full	Discov. rate	t discov.
Tetrahedron	24	1500 s	16.7 %	390 s
Hexahedron	48	3203 s	14.5 %	419 s
Octahedron	36	1924	13.9 %	334 s
Icosahedron	72	4447	18.3 %	370 s
Icosphere Lv1	120	7454	16.7 %	341 s
Icosphere Lv2	252	14913	19.4 %	304 s

orien. - # of assembly orientation; t full - Time cost to explore all the orientation; Discov. rate - success rate to find feasible assembly motion; t discov. - The time cost before finding feasible assembly motion by random search. The time costs and discovery rates in the table are the mean of ten simulation. The different orientations used in Table V are as follows. From left to right: Tetrahedron, Hexahedral, Icosahedron, Icosphere Lv1, Icosphere Lv2.



ers may find some other examples in the attached video.

TABLE VI: Comparison of the two selection orders

Process	# of sampled grasps (right · left)				
	200 · 234	256 · 348	320 · 456	420 · 614	596 · 772
CD1	20 s	22 s	34 s	41 s	63 s
IK1	9 s	11 s	20 s	23 s	41 s
RRT1	33 s	32 s	36 s	39 s	43 s
CD2	8	10 s	16 s	20 s	36 s
IK2	5 s	5 s	9 s	9 s	17 s
RRT2	15 s	14 s	15 s	17 s	27 s
SUM	90 s	94 s	130 s	149 s	227 s

The time costs in the table are the mean of ten times of simulation.

VII. CONCLUSIONS

A dual-arm assembly planner to assemble multiple objects considering gravitational constraints is developed. The planner selects grasp configurations and assembly poses, as well as plans robot motion, considering gravity. It automatically picks upward poses to assemble the second part, and rotates the finished part considering gravity constraints to avoid dropping. Experiments and analysis showed the proposed planner is able to optimize the poses and motion for safe assembly. The planner is proved to be robust and efficient for dual-arm assembly planning.

REFERENCES

- [1] T. De Fazio and D. Whitney, "Simplified generation of all mechanical assembly sequences," *IEEE Journal on Robotics and Automation*, vol. 3, no. 6, pp. 640–658, 1987.
- [2] L. H. De Mello and A. C. Sanderson, "And/or graph representation of assembly plans," *IEEE Transactions on robotics and automation*, vol. 6, no. 2, pp. 188–199, 1990.
- [3] R. H. Wilson and J.-C. Latombe, "Geometric reasoning about mechanical assembly," *Artificial Intelligence*, vol. 71, no. 2, pp. 371–396, 1994.
- [4] A. C. Sanderson, "Assemblability based on maximum likelihood configuration of tolerances," *IEEE Transactions on Robotics and Automation*, vol. 15, no. 3, pp. 568–572, 1999.
- [5] R. A. Knepper, T. Layton, J. Romanishin, and D. Rus, "Ikeabot: An autonomous multi-robot coordinated furniture assembly system," in *IEEE International Conference on Robotics and Automation*. IEEE, 2013, pp. 855–862.

- [6] P. Jiménez, "Survey on assembly sequencing: a combinatorial and geometrical perspective," *Journal of Intelligent Manufacturing*, vol. 24, no. 2, pp. 235–250, 2013.
- [7] R. Mattikalli, D. Baraff, P. Khosla, and B. Repetto, "Gravitational stability of frictionless assemblies," *IEEE Transactions on Robotics and Automation*, vol. 11, no. 3, pp. 374–388, 1995.
- [8] H. Dobashi, J. Hiraoka, T. Fukao, Y. Yokokohji, A. Noda, H. Nagano, T. Nagatani, H. Okuda, and K.-i. Tanaka, "Robust grasping strategy for assembling parts in various shapes," *Advanced Robotics*, vol. 28, no. 15, pp. 1005–1019, 2014.
- [9] M. Dogar, A. Spielberg, S. Baker, and D. Rus, "Multi-robot grasp planning for sequential assembly operations," in *IEEE International Conference on Robotics and Automation (ICRA)*. IEEE, 2015, pp. 193–200.
- [10] F. Suárez-Ruiz, X. Zhou, and Q.-C. Pham, "Can robots assemble an ikea chair?" *Science Robotics*, vol. 3, no. 17, p. eaat6385, 2018.
- [11] M. McEvoy, E. Komendera, and N. Correll, "Assembly path planning for stable robotic construction," in *IEEE International Conference on Technologies for Practical Robot Applications (TePRA)*. IEEE, 2014, pp. 1–6.
- [12] S. Ghandi and E. Masehian, "Review and taxonomies of assembly and disassembly path planning problems and approaches," *Computer-Aided Design*, vol. 67, pp. 58–86, 2015.
- [13] W. Wan, K. Harada, and K. Nagata, "Assembly sequence planning for motion planning," *Assembly Automation*, vol. 38, no. 2, pp. 195–206, 2018.
- [14] L. P. Kaelbling and T. Lozano-Pérez, "Integrated task and motion planning in belief space," *The International Journal of Robotics Research*, vol. 32, no. 9-10, pp. 1194–1227, 2013.
- [15] J. Wolfe, B. Marthi, and S. Russell, "Combined task and motion planning for mobile manipulation," in *Twentieth International Conference on Automated Planning and Scheduling*, 2010.
- [16] S. Srivastava, E. Fang, L. Riano, R. Chitnis, S. Russell, and P. Abbeel, "Combined task and motion planning through an extensible planner-independent interface layer," in *IEEE International Conference on Robotics and Automation (ICRA)*. IEEE, 2014, pp. 639–646.
- [17] C. Zhang and J. A. Shah, "Co-optimizing task and motion planning," in *IEEE/RSJ International Conference on Intelligent Robots and Systems*, 2016, pp. 4750–4756.
- [18] F. Lagriffoul, N. T. Dantam, C. Garrett, A. Akbari, S. Srivastava, and L. E. Kavraki, "Platform-independent benchmarks for task and motion planning," *IEEE Robotics and Automation Letters*, vol. 3, no. 4, pp. 3765–3772, 2018.
- [19] B. Siciliano, *Advanced bimanual manipulation: Results from the dexmart project*. Springer Science & Business Media, 2012, vol. 80.
- [20] H. A. Park and C. G. Lee, "Dual-arm coordinated-motion task specification and performance evaluation," in *IEEE/RSJ International Conference on Intelligent Robots and Systems (IROS)*. IEEE, 2016, pp. 929–936.
- [21] J.-P. Saut, M. Gharbi, J. Cortés, D. Sidobre, and T. Siméon, "Planning pick-and-place tasks with two-hand regrasp," in *IEEE/RSJ International Conference on Intelligent Robots and Systems*. IEEE, 2010, pp. 4528–4533.
- [22] W. Wan, H. Igawa, K. Harada, H. Onda, K. Nagata, and N. Yamanobe, "A regrasp planning component for object reorientation," *Autonomous Robots*, pp. 1–15, 2018.
- [23] L. Chen, L. F. Figueredo, and M. Dogar, "Manipulation planning under changing external forces," in *IEEE/RSJ International Conference on Intelligent Robots and Systems (IROS)*. IEEE, 2018, pp. 3503–3510.
- [24] B. Cohen, S. Chitta, and M. Likhachev, "Search-based planning for dual-arm manipulation with upright orientation constraints," in *IEEE International Conference on Robotics and Automation*. IEEE, 2012, pp. 3784–3790.
- [25] I. G. Ramirez-Alpizar, K. Harada, and E. Yoshida, "Human-based framework for the assembly of elastic objects by a dual-arm robot," *Robomech Journal*, vol. 4, no. 1, p. 20, 2017.
- [26] S. Stavridis and Z. Doulgeri, "Bimanual assembly of two parts with relative motion generation and task related optimization," in *IEEE/RSJ International Conference on Intelligent Robots and Systems (IROS)*. IEEE, 2018, pp. 7131–7136.
- [27] W. Wan and K. Harada, "Developing and comparing single-arm and dual-arm regrasp," *IEEE Robotics and Automation Letters*, vol. 1, no. 1, pp. 243–250, 2016.